Ecological Modelling 430 (2020) 109151

Contents lists available at ScienceDirect

Ecological Modelling

journal homepage: www.elsevier.com/locate/ecolmodel

Modeling the Growth of Sugar Kelp (*Saccharina latissima*) in Aquaculture Systems using Dynamic Energy Budget Theory

Celeste T. Venolia[a], Romain Lavaud[b], Lindsay A. Green-Gavrielidis[c,1], Carol Thornber[c], Austin T. Humphries[a,d,*]

[a] Department of Fisheries, Animal and Veterinary Sciences, University of Rhode Island, Kingston, Rhode Island
[b] Institut des Sciences de la Mer, Université du Québec à Rimouski, Rimouski, QC, Canada
[c] Department of Natural Resources Science, University of Rhode Island, Kingston, Rhode Island
[d] Graduate School of Oceanography, University of Rhode Island, Narragansett, Rhode Island

ARTICLE INFO

Keywords:
Macroalgae
Food production
Bioenergetics
Synthesizing units
Rhode Island

ABSTRACT

Aquaculture is an industry with the capacity for further growth that can contribute to sustainable food systems to feed an increasing global population. Sugar kelp (*Saccharina latissima*) is of particular interest for farmers as a fast-growing species that benefits ecosystems as a primary producer. However, as a new industry in the U.S., farmers interested in growing *S. latissima* lack data on growth dynamics. To address this gap, we calibrated a Dynamic Energy Budget (DEB) model to data from the literature and field-based growth experiments in Rhode Island (U.S.A.). Environmental variables forcing model dynamics include temperature, irradiance, dissolved inorganic carbon concentration, and nitrate and nitrite concentration. The modeled estimates for field *S. latissima* blade length were accurate despite underestimation of early season growth. In some simulations, winter growth was limited by the rate at which the light-dependent reaction of photosynthesis, the first step of carbon assimilation, was performed. Nitrogen (N) reserves were also an important limiting factor especially later in the spring season as irradiance increased, although the low resolution of N forcing concentrations might restrict the model accuracy. Since this model is focused on *S. latissima* grown in an aquaculture setting with winter and spring growth, no specific assumptions were made to include summer growth patterns such as tissue loss or reproduction. The results indicate that this mechanistic model for *S. latissima* captures growth dynamics and blade length at the time of harvest, thus it could be used for spatial predictions of *S. latissima* aquaculture production across a range of environmental conditions and locations. The model could be a particularly useful tool for further development of sustainable ocean food production systems involving seaweed.

1. Introduction

Aquaculture is currently the fastest growing food production sector in the world and is likely to become the main seafood supply in the future (FAO, 2018). In open systems of fed species, aquaculture activities can cause concentrated fluxes of feces and feed wastage leading to eutrophication (Wu, 1995) and alteration of food webs (Herbeck et al., 2013). Open aquaculture systems composed of species that do not require supplemental feed or nutrients (i.e., primary producers and filter feeders) avoid these harms and instead can provide important ecosystem services such as removing dissolved organic and inorganic nutrients (Alleway et al., 2019). Seaweeds are of particular interest as they mitigate hypoxia from terrestrial food production systems and even protect shorelines through dampening of wave energy (Duarte et al., 2017). Outside of these ecosystem services, growing seaweed has been proposed as a way to engage a wider public audience with climate change via offsetting carbon emissions (Froehlich et al., 2019). Seaweed aquaculture has the potential to generate net positive environmental and social impacts, but this industry has been traditionally concentrated in Asian countries (FAO, 2018).

The U.S. does not produce enough aquatic plants to even register in the global production statistics (< 0.1%; FAO, 2018). In the Northeast U.S., sugar kelp (*Saccharina latissima*) is a local species of recent interest for food, biofuel, bioremediation, and pharmaceutical products (Forbord et al., 2012). In a single season of aquaculture growth, *S. latissima* blades can grow up to 60-140 cm depending on the water depth,

* Corresponding Author.
E-mail address: humphries@uri.edu (A.T. Humphries).
[1] Present address: Department of Biology and Biomedical Sciences, Salve Regina University, Newport, RI, USA

https://doi.org/10.1016/j.ecolmodel.2020.109151
Received 1 February 2020; Received in revised form 20 May 2020; Accepted 23 May 2020
Available online 31 May 2020
0304-3800/

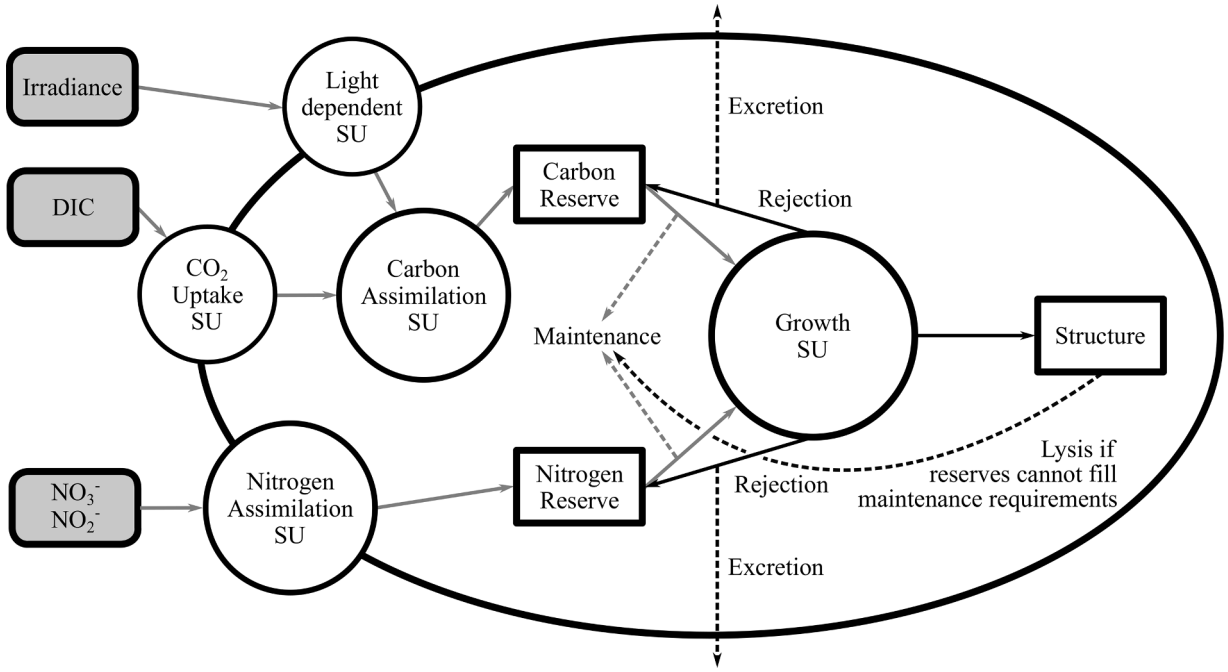

Fig. 1. *S. latissima* DEB model conceptual framework (adapted from Lavaud et al., 2020). The large oval represents the algae and the surrounding area is its environment. Grey rounded rectangles are the model forcing variables. White rectangles are the state variables of the model, representing the main pools of mass in the modeled organism. Circles are synthesizing units, processing key metabolic transformations. Dotted arrows represent fluxes of mass leaving the main model system either through excretion or use in maintenance. Grey arrows depict where the temperature correction is applied to a reaction.

planting time, and nutrient availability (Handå et al., 2013). Oysters, however, are the most widely aquacultured species in coastal areas of the U.S (NMFS, 2018). The Eastern oyster (*Crassostrea virginica*) mostly grows during the summer months when water temperatures are above 15 °C and is in a state of relative dormancy in the winter (Dame, 1972). It has been suggested that cultivation of *S. latissima* could complement oyster farming because of the differences in growing season with kelp growing mainly when water temperatures are below 15 °C. Therefore, kelp could provide an additional source of income without interfering with oyster production. This new industry, however, would benefit from production estimates in order to assess the biological and economic sustainability of *S. latissima* farming.

Bioenergetic models can provide such production estimates by studying energy fluxes and usage between the environment and the organism and within the organism. They constitute useful tools in the early development of an aquaculture activity to: assess the carrying capacity of a system before installing new farms (Grant et al., 2007; Filgueira et al., 2014), estimate production and feeding ration (Cho and Bureau, 1998), or to optimize integrated multi-trophic aquaculture (IMTA) systems (Ren et al., 2012). Forcing variables in bioenergetic modelling frameworks are of prime importance as they define the system response. In the case of *S. latissima*, blade growth is mainly influenced by irradiance, temperature, and nutrient concentration (Boden, 1979). Other factors such as wave action (Buck and Buchholz, 2005) and ambient light regime (Gerard, 1988) may also determine growth dynamics. In a simple predictive model, Petrell et al. (1993) estimated growth of *S. latissima* using a linear relationship with dissolved inorganic nitrogen concentration and a temperature correction. This model required an assumption that nitrogen dynamics are always limiting growth, thus ignoring the potential influence of irradiance. While integrating photosynthetic processes into a model can be challenging, mechanistic approaches may be more suited to capture the physiological response to environmental variability, especially in a changing environment (Denny and Helmuth, 2009).

Dynamic energy budget (DEB) theory provides a sound mechanistic basis for understanding an organism's energetics, which is used to model the flow of mass and energy through an organism from uptake to usage for maintenance, growth, reproduction, or excretion (Kooijman, 2010). This theory of metabolic organization provides a framework to examine the interactive effects of environmental nutrient concentrations and irradiance on an organism through parallel systems of nitrogen (N) and carbon (C) dynamics. Modeling autotrophs is a less common direction for the application of DEB theory. Thus, multiple reserves are necessary to accurately model matter and energy dynamics because of the different nutrient uptake pathways (Kooijman, 2010). Autotroph DEB models have been constructed for microalgae (Lorena et al., 2010, Livanou et al., 2019), phytoplankton-zooplankton interactions (Poggiale et al., 2010), calcification of a coccolithophore (Muller and Nisbet, 2014), and recently the macroalga *Ulva lactuca* (Lavaud et al., 2020). Broch and Slagstad (2012) were the first to develop a dynamic bioenergetic model for *S. latissima*, borrowing concepts from DEB theory with the aim of creating a tool for optimizing aquaculture production of Norwegian *S. latissima*. These authors based their model structure on a Droop's cell quota model completed by numerous empirical and allometric relationships to simulate growth of *S. latissima,* but this simplification did not increase parsimony (i.e., reduce the number of model parameters). Using a DEB framework, however, ensures theoretical coherence (i.e., mechanistic description of metabolic processes) and ease of model transference to other regions through less re-calibration.

Our objective with this study is to develop a bioenergetic model for *S. latissima* growth using the mechanistic properties of DEB theory. Specifically, we aim to calibrate the macroalga DEB model presented by Lavaud et al. (2020) to field data on kelp from Rhode Island (U.S.A.). The application of this model to another species from a different environment constitutes an important step in the validation of this model structure. The resulting model allows for growth predictions based on environmental inputs and has the potential to support the sustainable aquaculture industry, particularly with regard to site selection.

Table 1
Model equations with environmental conditions: T = temperature (K), I = irradiance (mol γ m^{-2} h^{-1}), DIC = dissolved inorganic carbon (mol DIC L^{-1}), and N = nitrate and nitrite concentration (NO_3^- and NO_2^- L^{-1}).

Equation	Description
$C_T = exp(\frac{T_A}{T_0} - \frac{T_A}{T})[1 + exp(\frac{T_{AL}}{T_0} - \frac{T_{AL}}{T_L}) + exp(\frac{T_{AH}}{T_H} - \frac{T_{AH}}{T_0})]$ $[1 + exp(\frac{T_{AL}}{T} - \frac{T_{AL}}{T_L}) + exp(\frac{T_{AH}}{T_H} - \frac{T_{AH}}{T})]^{-1}$	Temperature correction
$j_{E_N A} = j_{E_N Am} C_T \frac{[N]}{[N]+K_N}$	Specific assimilation rate of N
$j_{CO_2} = j_{CO_2 m} C_T \frac{[DIC]}{[DIC]+K_C}$	Specific CO_2 uptake rate from photosynthetic SU1
$j_I = \frac{\rho_{PSU} Ib_I \alpha_I}{1 + \frac{Ib_I \alpha_I}{k_I C_T}}$	Specific relaxation rate from photosynthetic SU2
$j_{O_2} = \frac{M_V}{w_d} j_I y_{LO_2} w_{O_2}$	Oxygen production rate
$j_{E_C A} = (\frac{1}{j_{E_C Am} C_T} + \frac{1}{j_{CO_2}/y_{CO_2 C}} + \frac{1}{j_I/y_{IC}} - \frac{1}{j_I/y_{IC} + j_{CO_2}/y_{CO_2 C}})^{-1}$	Specific assimilation rate of C from photosynthetic SU3
$j_{E_i C} = m_{E_i}(\dot{k}_{Ei} C_T - \dot{r})$	Specific catabolic flux of N or C reserve
$\dot{r} = \frac{1}{M_V}\frac{dM_V}{dt}$	Net specific growth rate
$j_{E_i}^{M_i} = \min(j_{E_i C}, j_{E_i M} C_T)$	Specific maintenance flux from N or C reserve
$j_{E_i G} = j_{E_i C} - j_{E_i}^{M_i}$	Specific growth flux from N or C reserve
If $j_{E_i}^{M_i} < j_{E_i M} C_T$	Specific maintenance flux from structure
$j_V^M = \sum_i j_{V_i}^{M_i} = \sum_i [(j_{E_i M} C_T - j_{E_i}^{M_i}) y_{E_i V}^{-1}]$	
$j_{VG} = [\sum_i (\frac{j_{E_i G}}{y_{E_i V}})^{-1} - (\sum_i \frac{j_{E_i G}}{y_{E_i V}})^{-1}]^{-1} = \dot{r} + j_V^M$	Gross specific growth rate
$j_{E_i R} = j_{E_i G} - y_{E_i V} j_{VG}$	Specific flux of rejected C or N from growth SU
$\frac{d}{dt} m_{E_i} = j_{E_i A} - j_{E_i C} + \kappa_{E_i} j_{E_i R} - \dot{r} m_{E_i}$	Dynamics of the N or C reserve
$\frac{d}{dt} M_V = \dot{r} M_V$	Dynamics of structural mass
$W_d = (w_V + m_{E_C} w_{EC} + m_{E_N} w_{EN}) M_V$	Whole *S. latissima* blade dry weight
$L_w = (\frac{W_d}{3.87\ 10^{-3}})^{\frac{1}{1.469}}$	Physical length

2. Methods

2.1. Dynamic energy budget model assumptions

The *S. latissima* model is based on a DEB model developed for sea lettuce by Lavaud et al. (2020). The core structure of the *S. latissima* model tracks the uptake of carbon (C) and nitrogen (N), their assimilation into specific reserves and allocation to growth or maintenance or their excretion (Fig. 1). The variables that depict the state of the model are the mass of structure M_V (in mol V, moles of structure), Nitrogen reserve density m_{E_N} (in mol N per mol V), and Carbon reserve density m_{E_C} (in mol C per mol V). The code for this model is freely available at https://github.com/CVenolia/SugarKelpDEB.

A core assumption of DEB theory, strong homeostasis, maintains that reserve and structure have constant chemical compositions (Kooijman, 2010). This does not mean that there are always constant amounts of reserve and structure; rather, the amount of carbon, nitrogen, hydrogen, and oxygen relative to each other within specific reserves or structures remains constant.

Two substrates and associated reserves were considered in this *S. latissima* model: C and N (nitrate and nitrite, collectively); other potential nutrients such as phosphorous or potassium were dismissed based on the fact that in regions where nitrogen is not abundant year-round, nitrogen availability is what drives accelerated growth in winter and early spring (Gagné et al., 1982). Adding further reserves to the model would increase complexity by increasing the number of state variables and parameters with potentially little to no increase in accuracy. On the C side of the model, since *S. latissima* and other algae use carbonic anhydrase to assimilate bicarbonate and convert it into carbon dioxide (Axelsson et al., 2000), we assumed that assimilating carbon dioxide directly was identical to assimilating carbon dioxide that was formed extracellularly from bicarbonate through a carbon concentrating mechanism.

Another assumption of this DEB model is that *S. latissima* is a V1-morph. In DEB theory, V1-morphs are organisms whose surface area is proportional to volume (Kooijman, 2010). *S. latissima* grows as a sheet in both length and width directions at the meristematic blade region near the stipe (Sjøtun, 1993). Variation in blade thickness over an individual blade and through time does not have a substantial impact on the surface area to volume ratio (Vettori and Nikora, 2017) to preclude the V1-morph assumption. Drag from water speed has been found to impact blade morphology (Buck and Buchholz, 2005) but this difference in appearance should not affect the surface area to volume ratio either.

Other assumptions were grounded in the fact that this model was used to determine aquaculture production, which is currently limited in time to November-May. Energy was not used for reproduction or maturity in this model, a simplification that allows for a more parsimonious model. There is evidence suggesting that kelp produces inhibitors that minimize the formation of reproductive tissue during the rapid growth phase (Buchholz and Lüning, 1999, Lüning et al., 2000). Moreover, only a small subset of blades show reproductive development by the time the aquaculture harvest occurs in spring, towards the end of the first period of rapid growth. Furthermore, the aquaculture season of *S. latissima* is set up to maximize growth while minimizing loss or degradation of tissues due to various stresses. Apical frond loss in kelp is correlated with temperature stress and wave action (Krumhansl et al., 2014), mechanical stress of biofouling (Brown et al., 1997), and overall blade length (Sjøtun, 1993). A tissue loss function would be necessary to accurately model *S. latissima* growth year-round, however, the exact mechanism for this loss remains context-specific in the literature. Aquaculture farmers generally harvest kelp before

Table 2
S. latissima DEB model parameters and units resulting from fitting the model to the compiled literature and field data.

Parameter	Parameter description	Parameter Units	Value	Source
$\dot{j}_{E_N Am}$	Maximum volume specific nitrogen assimilation	mol N mol V^{-1} h^{-1}	1.5 * 10^{-4}	Fitted from data by Espinoza and Chapman (1983)
K_N	Half-saturation concentration for NO_3^- and NO_2^- uptake	mol NO_3^- and NO_2^- L^{-1}	2.5 * 10^{-6}	Fitted from data by Espinoza and Chapman (1983)
$\dot{j}_{CO_2 m}$	Maximum volume specific CO_2 uptake rate	mol CO_2 mol V^{-1} h^{-1}	0.0075	This study
K_C	Half-saturation concentration for CO_2 uptake	mol CO_2 L^{-1}	4 * 10^{-7}	This study
ρ_{PSU}	Photosynthetic unit (PSU) density	mol PSU mol V^{-1}	0.5	Fitted from data by Johansson and Snoeijs (2002)
$\dot{b}_I$	Binding probability of a photon to a free light SU	-	0.5	Fitted from data by Johansson and Snoeijs (2002)
α_I	Specific photon arrival cross section	m^2 mol PSU^{-1}	1	Fitted from data by Johansson and Snoeijs (2002)
$\dot{k}_I$	Dissociation rate of photosynthetic products	mol γ mol PSU^{-1} h^{-1}	0.075	Fitted from data by Johansson and Snoeijs (2002)
y_{IC}	Yield of C reserve per photon	mol γ mol C^{-1}	10	Lavaud et al. (2020)
$y_{CO_2 C}$	Yield of C reserve per CO_2	mol CO_2 mol C^{-1}	1	Lavaud et al. (2020)
y_{LO_2}	Yield factor of photon to O_2	mol O_2 mol γ $^{-1}$	0.125	Lavaud et al. (2020)
$\dot{j}_{E_C Am}$	Maximum volume specific carbon assimilation	mol C mol V^{-1} h^{-1}	0.282	This study
$\dot{k}_{EN}$	N reserve turnover rate	h^{-1}	0.04	Lavaud et al. (2020)
$\dot{k}_{EC}$	C reserve turnover rate	h^{-1}	0.02	Lavaud et al. (2020)
$\dot{j}_{E_N M}$	Volume specific maintenance cost paid by N reserve	mol N mol V^{-1} h^{-1}	4 * 10^{-6}	This study
$\dot{j}_{E_C M}$	Volume specific maintenance cost paid by C reserve	mol C mol V^{-1} h^{-1}	1 * 10^{-6}	This study
$y_{E_N V}$	Yield factor of N reserve to structure	mol N mol V^{-1}	0.04	Lorena et al. (2010)
$y_{E_C V}$	Yield factor of C reserve to structure	mol C mol V^{-1}	1	This study
κ_{E_i}	Fraction of rejection flux incorporated back in i-reserve	-	0.9	This study
T_A	Arrhenius temperature	K	6314.3	This study
T_0	Reference temperature	K	293.15	This study
T_H	Upper boundary of temperature tolerance	K	286.536	This study
T_L	Lower boundary of temperature tolerance	K	273.15	This study
T_{AH}	Arrhenius temperature outside T_H	K	18702	This study
T_{AL}	Arrhenius temperature outside T_L	K	4391.9	This study
w_V	Molar weight of structure	g mol V $^{-1}$	29.89	C:H:O:N; 1: 1.33:1:0.04
w_{EC}	Molar weight of C reserve	g C mol C^{-1}	54	C:H:O:N; 1:2:1:0
w_{EN}	Molar weight of N reserve	g N mol N^{-1}	17	C:H:O:N; 0:0:2.5:1
w_{O_2}	Molar weight of O_2	g O_2 mol O_2^{-1}	32	Periodic table

biofouling begins, which maximizes harvestable blade length and product quality. Photoinhibition may occur in *S. latissima* when high light conditions are combined with high temperature conditions (Heinrich et al., 2012), but since we limit the application of our model to winter-spring seasons, photoinhibition was not accounted for. Photorespiration was not included either to simplify model dynamics (Kooijman, 2010).

2.2. Model structure

All the equations for this model are based on and detailed in Lavaud et al. (2020; Table 1). *S. latissima* blade length (L_w) was calculated via total dry weight (W_d) using an allometric relationship proposed by Gevaert et al. (2001; Table 1). The change in the three state variables (reserve density of C and N and mass of structure) over time is described by differential equations that where solved using the deSolve package (Soetaert et al., 2010) in R (R Core Team, 2019).

2.3. Model calibration

The parameters of the *S. latissima* DEB model were manually calibrated to fit simultaneously a combination of literature data and field data collected for this study (Table 2). Root mean square error (RMSE) was used as a measure of spread in the residuals for assessing the quality of model predictions compared to each observation data set.

2.3.1. Literature data

Information about the locations where literature studies were conducted was also included because there are multiple ecotypes of *S. latissima* (Gerard, 1988), which may influence their physiological response (Table 3). Due to a lack of local information on certain aspects of *S. latissima* life history traits, this model was calibrated with data across multiple ecotypes of *S. latissima*. The Arrhenius relationship parameters were estimated using a least squared non-linear regression on compiled physiological rates from the literature. Prior to the estimation, each data set was standardized by dividing by the averaged value found at the reference temperature (Table 3). The nitrate and nitrite uptake parameters, $\dot{j}_{E_N Am}$ maximum volume specific nitrogen assimilation and K_N half-saturation concentration for NO_3^- and NO_2^- uptake, were calibrated using nitrate uptake data from Espinoza and Chapman (1983). To match the dimensions used by these authors (μmol N^{-1} g_{DW}^{-1} h^{-1}) the volume-specific modeled N uptake was multiplied by M_V/W_d (structural mass divided by dry weight). Photosynthesis parameters, ρ_{PSU} photosynthetic unit (PSU) density, α_I specific photon arrival cross section, $\dot{b}_I$ binding probability of a photon to a free light synthesizing unit, and $\dot{k}_I$ dissociation rate of photosynthetic products, were calibrated using oxygen production data from Johansson and Snoeijs (2002).

Appropriate literature data for calibrating several model parameters were not available. For instance, air-based carbon dioxide uptake data for *S. latissima* (Ní Longphuirt et al., 2013) were examined to estimate dissolved inorganic carbon uptake but ultimately were rejected due to likely dissimilarity to submerged uptake. Carbon uptake parameters, maintenance rates, the yield factor of C reserve and the rejection flux were estimated during model testing so as to result in predicted length within the observed range in length data (Table 2). Other parameters such as the reserve turnover rates are difficult to compare to measurable physiological data, so these parameters were set based on previously assumed values by Lorena et al. (2010) and Lavaud et al. (2020).

2.3.2. Field data

S. latissima was grown at four oyster farm sites from fall to spring in both 2017-2018 (Year 1) and 2018-2019 (Year 2). *S. latissima* seed was raised in aquaria from harvested local reproductive *S. latissima* tissue collected at Ft. Wetherill, RI, following the methods of Redmond et al. (2014), and seed lines were attached to ropes held in

Table 3
Data from literature and this study used to calibrate the *S. latissima* DEB model.

Reference	Location	Data	Experimental conditions	Time period
Espinoza and Chapman (1983)	Nova Scotia, Canada	NO_3^- uptake (μg N g_{DW}^{-1} h^{-1})	T = 9 and 18°C [N] = from 2.5 to 88 * 10^{-6} M NO_3^-	Discrete measurements
Johansson and Snoeijs (2002)	Sweden	Measured O_2 evolution (μmol O_2 kg DW^{-1} s^{-1})	T = 14°C I = 0-900 μE m^{-2} s^{-1}	Discrete measurements
*Davison (1987)	Germany	Photosynthesis rates (μmol C g_{WW}^{-1} h^{-1})	T = 0-30°C with 5°C intervals I = 200 μE m^{-2} s^{-1}	Discrete measurements
*Fortes and Lüning (1980)	Germany	Specific growth rate (% d^{-1})	T = 0, 5, 10, 15, and 20°C I = 70 μE m^{-2} s^{-1}	7 days
*Bolton and Lüning (1982)	Germany, UK, France, and Norway	Specific growth rate (% d^{-1})	T° = 0, 5, 10, 15, 20, and 23°C I = 50 μE m^{-2} s^{-1}	7 days
*Davison and Davison, 1987	Germany	Relative growth rate (cm cm^{-1} $month^{-1}$)	T = 0, 5, 10, 15 and 20°C I = 60 μE m^{-2} s^{-1}	1 month
This study	Rhode Island, USA	Blade length (cm) and N:C ratio (mol mol^{-1})	T = 1.5-20°C [N] = 0-1 * 10^{-5} mol NO_3^- and NO_2^- L^{-1} [C] = 1.836 * 10^{-3} mol DIC L^{-1} at Pt. Judith Pond sites and 1.956 * 10^{-3} mol DIC L^{-1} for Narragansett Bay sites I = 0-2 * 10^6 daily μE m^{-2} h^{-1}	138- 172 days

* Used only to build the Arrhenius relationship.

place by moorings at each of the farms. The growing sites were split between Narragansett Bay and Pt. Judith Pond, RI (Fig. 2). Longlines of *S. latissima* were placed in duplicates at a depth of 1 m at all the growing sites. *S. latissima* growth, measured as length and width (cm), was monitored every 20-85 days using a subset of individuals harvested from the longline. The variability in monitoring timing was largely driven by the availability of farmers to assist with logistics as well as weather conditions.

Temperature data were collected every fifteen minutes at each site using HOBO® pendant loggers. Water samples were collected when *S. latissima* growth measurements were taken to determine the concentrations of nitrate and nitrite. In year 1, nitrate and nitrite concentrations were measured using a LACHAT Flow Injection Autoanalyzer (LACHAT, 2008, method detection limit 0.3 μM). In year 2, nitrate and nitrite concentrations were determined using an Astoria Pacific Model 303A Segmented Continuous Flow Autoanalyzer (Astoria-Pacific Inc, Clackamas, OR; Eaton et al., 1998, method detection limit 1.43 μM). Because Narragansett Bay S data were below the method detection limit for the analysis done in year 2, we replaced them with data from the nearby University of Rhode Island Graduate School of Oceanography to better reflect reality; samples were run on an Astoria Analyzer (Reed and Oviatt, 2020, method detection limit of 0.1 μM).

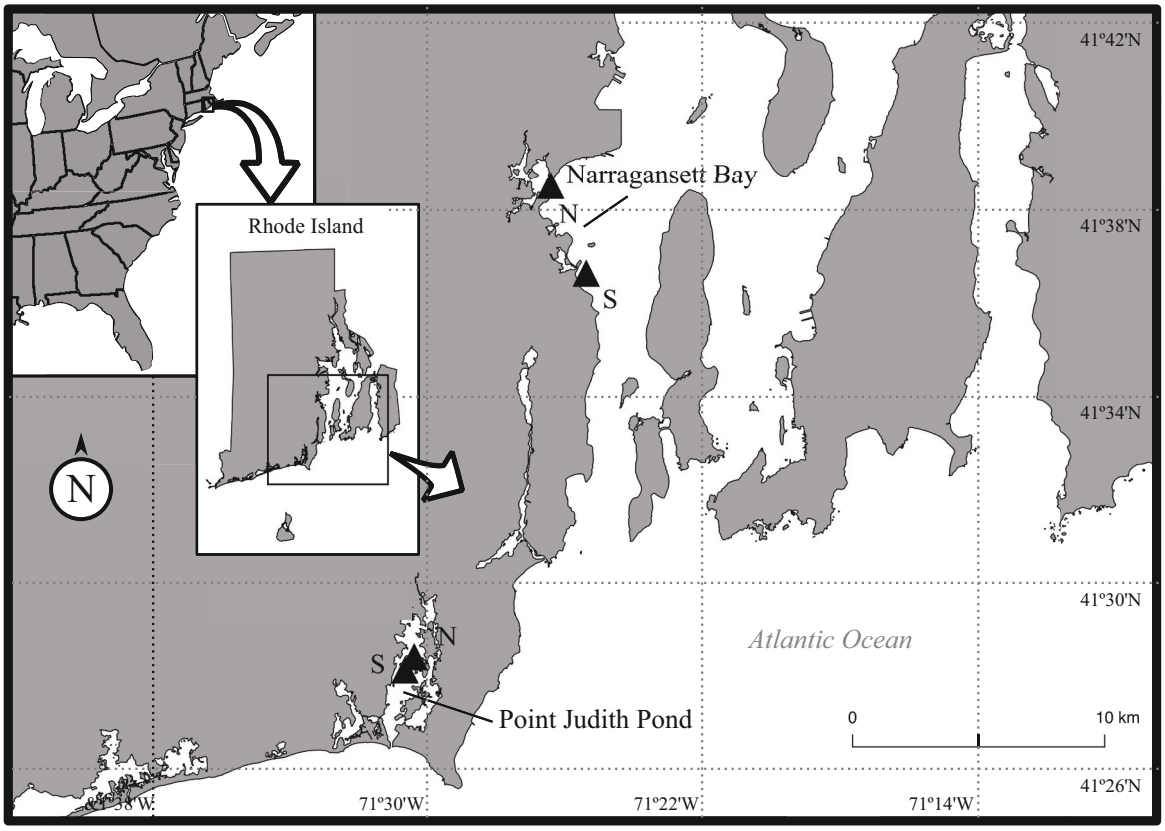

Fig. 2. Map of growing sites (triangles) for *S. latissima* on Rhode Island oyster farms.

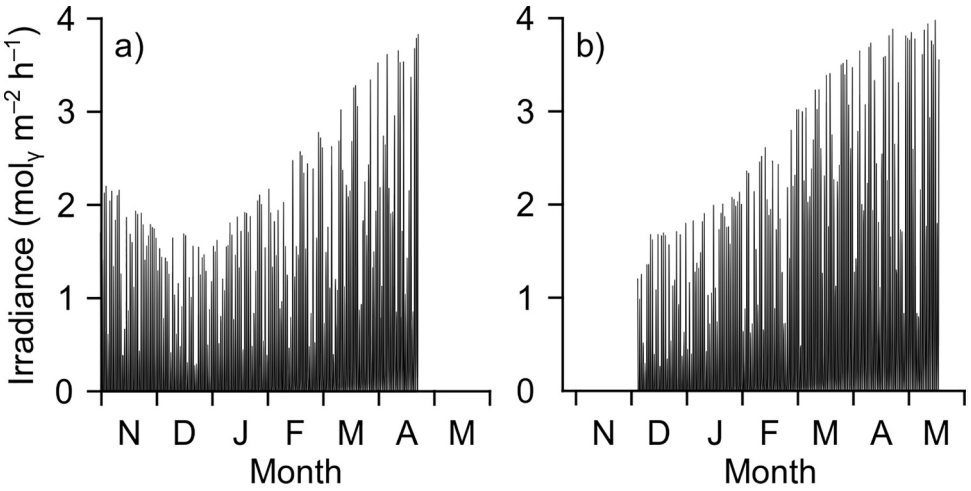

Fig. 3. Irradiance forcing used in all sites for year 1 (a) and year 2 (b) of the field study converted from the radiative forcing from the North American Regional Reanalysis.

2.4. Model forcing

The *S. latissima* model was forced with temperature, irradiance, dissolved inorganic carbon (DIC) concentration, and nitrate and nitrite concentration data on an hourly time step. Temperature recorded at fifteen-minute intervals at each site was averaged on an hourly basis. Due to difficulties with biofouling on irradiance loggers, we used radiative forcing from the North American Regional Reanalysis (Mesinger et al., 2006) to estimate photosynthetically active radiation (PAR, mol γ m^{-2} h^{-1} or E m^{-2} h^{-1}) using this equation: PAR = NSW*PAR_{frac}*C*$e^{(-k * z)}$*3600, with *NSW* the net shortwave radiation (W m^{-2}) at the water surface calculated from downward shortwave flux minus upward shortwave flux, PAR_{frac} the fraction of the incident flux useable for photosynthesis (dimensionless), *C* a conversion factor (µmol γ s^{-1} W^{-1}), *k* extinction coefficient (m^{-1}), *z* line depth (m), and 3600 to convert from per second to per hour. We used a value of 4.56 µmol γ s^{-1} W^{-1} for C (Mõttus et al., 2011), a PAR_{frac} of 0.43 (Mõttus et al., 2011), a *k* of 0.46 m^{-1} from past work in Narragansett Bay (Ullman and Codiga, 2010), and a *z* of 1 m as kelp lines were held at a depth of a minimum of 1 m. We used linear interpolation to create an hourly forcing from source data every three hours (Fig. 3). All sites had the same base irradiance forcing in one year using this method. DIC concentration data were not collected in this study, so this forcing was estimated from other sources. The Pt. Judith Pond sites were held at a constant DIC value of 1.836 10^{-3} mol DIC L^{-1} based on U.S. Environmental Protection Agency data from Ninigret Pond (J. Grear, unpublished data). The Narragansett Bay sites were held at a constant DIC value of 1.956 10^{-3} mol DIC L^{-1} based on data from Brenton Point (Segarra, 2002). Nitrate and nitrite concentrations were also linearly interpolated on an hourly basis. State variable initial conditions were estimated based on approximate length and weight at planting of the kelp blades (M_V = 0.00164 g_{DW}). Reserve densities had to be assumed but their impact on end results is limited to the first few days of the simulation. Initial m_{E_C} was set at 0.002 mol C mol V^{-1} and m_{E_N} at 0.01 mol N mol V^{-1} in year 1 and 0.01 and 0.09, respectively, in year two.

2.5. Sensitivity analyses

To determine how each DEB parameter influenced simulation outputs, we analyzed the local sensitivity of the three state variables to model parameters using an L1 summary value of sensitivity from the R package FME (Soetaert and Petzoldt, 2010). The larger the L1 metric a parameter has the greater the sensitivity of the state variables to that parameter.

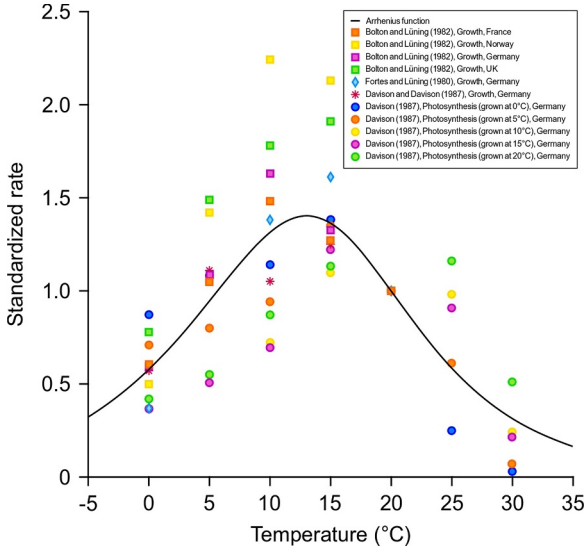

Fig. 4. Arrhenius relationship for *S. latissima* estimated using multiple growth and photosynthesis datasets from: Bolton and Lüning (1982; squares; orange for kelp from France, yellow for Norway, purple for Germany, green for the UK), Fortes and Lüning (1980; blue diamonds), Davison and Davison, 1987 (red asterisk), and Davison (1987 circles; blue for sporophytes rearing temp 0°C, orange for 5°C, yellow for 10°C, purple for 15°C, and green for 20°C). The adjusted R-squared statistic for the fit of the curve to the data points is 0.551 (p-value = 2.74 10^{-11}).

3. Results

3.1. Model calibration: literature data

The Arrhenius relationship fit to the compiled literature data (Table 3) reflected maximum physiological rates at temperatures around 13°C (Fig. 4). The lower boundary of the temperature tolerance range in the Arrhenius relationship was 0°C, and the upper boundary was 13.39°C. The rather low value for the upper boundary indicates that the optimum temperature is close to the upper limit of the tolerance range for this species. However, the shape of the curve past this point implies that the effects of high temperatures on the metabolism of sugar kelp appear gradually with increasing temperature. The adjusted R-squared for this relationship was 0.55 (p-value = 2.74 * 10^{-11}).

Using the nitrate uptake data from Espinoza and Chapman's (1983) St. Margaret's Bay site (Nova Scotia, Canada) provided estimates of

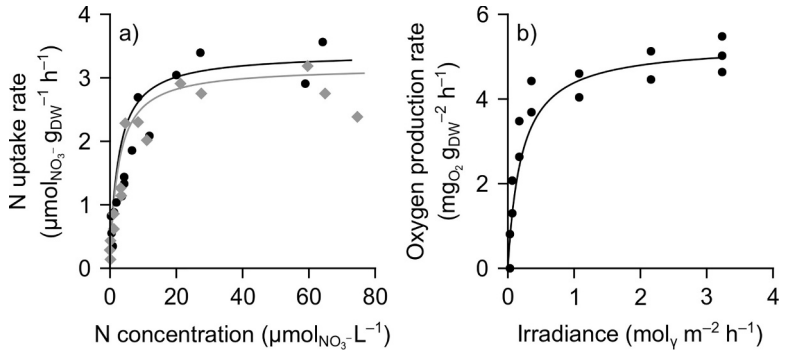

Fig. 5. Predicted (lines) and observed (points) a) N uptake from Espinoza and Chapman (1983) at 9°C (black circles) and 18°C (grey diamonds) and b) Oxygen production from Johansson and Snoeijs (2002).

maximum volume specific nitrate and nitrite assimilation of 1.5 * 10^{-4} mol N mol V^{-1} h^{-1} and a half-saturation concentration of 2.5 * 10^{-6} mol NO_3^- and NO_2^- L^{-1} (Fig. 5). The fit for the data collected at 18°C was slightly better with a RMSE of 0.374 μmol N g_{DW}^{-1} h^{-1} than the 9°C data at 0.504 μmol N g_{DW}^{-1} h^{-1}.

For the oxygen production data (Johansson and Snoeijs, 2002) used to calibrate the photosynthesis parameters, the values that had the lowest error around the data were a PSU density ρ_{PSU} = 0.05 mol PSU mol V^{-1}, specific photon arrival cross section α_I of 1 m^2 mol PSU^{-1}, a binding probability of a photon to a free light synthesizing unit $\dot{b}_I$ = 0.5 (dimensionless), and a dissociation rate of photosynthesis products $\dot{k}_I$ = 0.075 mol γ mol PSU^{-1} h^{-1} (Fig. 5). The resulting RMSE for this data set was 0.54 mg O_2 g_{DW}^{-1} h^{-1}. The maximum oxygen production rate of the model was approximately 4.95 mg O_2 g_{DW}^{-1} h^{-1} (Fig. 5).

3.2. Model calibration: field data

In year 1, the maximum water temperature recorded at the sites was 16.7°C in November and the minimum temperature was –1.72°C in January (Fig. 6). For year 2, the maximum temperature was 15.28°C in May and the minimum temperature was –1°C in January. Temperature changes were consistent across all four sites for both years.

The nitrate and nitrite concentration forcing variable had a lower resolution than the temperature forcing because of the linear interpolation between the N measurements (Fig. 6). The mean N concentration at the Pt. Judith Pond sites was 4.42 * 10^{-6} mol NO_3^- and NO_2^- L^{-1} (± 2.76 * 10^{-6}) and 2.20 * 10^{-6} mol NO_3^- and NO_2^- L^{-1} (± 2.99 * 10^{-6}) at the Narragansett Bay sites in year 1. For year 2, the mean N concentration at the Pt. Judith Pond sites was 1.01 * 10^{-6} mol NO_3^- and NO_2^- L^{-1} (± 2.11 * 10^{-6}) and 1.87 * 10^{-6} mol NO_3^- and NO_2^- L^{-1} (± 2.97 * 10^{-6}) at the Narragansett Bay sites.

3.3. Predicted growth and model dynamics

S. latissima grew quickly with mean elongation across all sites studied of 0.87 ± 0.63 cm d^{-1} in year 1 and 1.18 ± 0.62 cm d^{-1} in year 2 (Fig. 7). End of season blade length varied, but no clear trend based on sites was observed (Table 4). The *S. latissima* DEB model generally underestimated growth observed in the early parts of the season (planting to end of March) but accurately predicted the length at harvest within one standard deviation of the observed mean length for the majority of sites (Fig. 7). An exception to this trend was the first *S. latissima* line planted at Pt. Judith Pond South in year 1 for which final length was overestimated. The RMSEs for the model length prediction

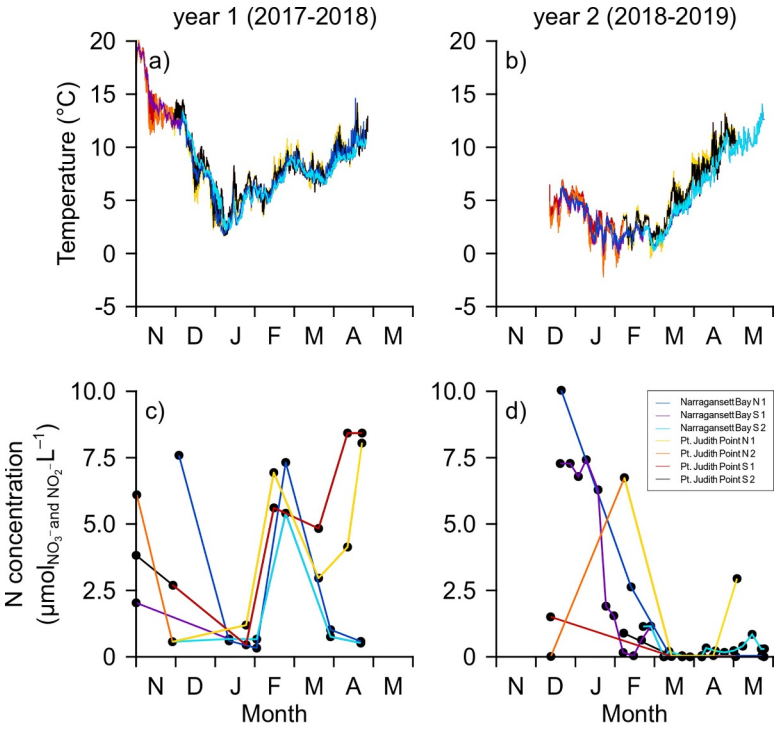

Fig. 6. Measured temperature (°C; a,b) and nitrate and nitrite concentrations (μmol L^{-1}; c,d) from year 1 (left panels) and year 2 (right panels). Narragansett Bay lines are in dark blue (North site 1), purple (South site 1), and light blue (South site 2). Pt. Judith Pond lines are in orange (North site 1), yellow (North site 2), brown (South site 1) and black (South site 2). Observed N concentrations are indicated by black dots.

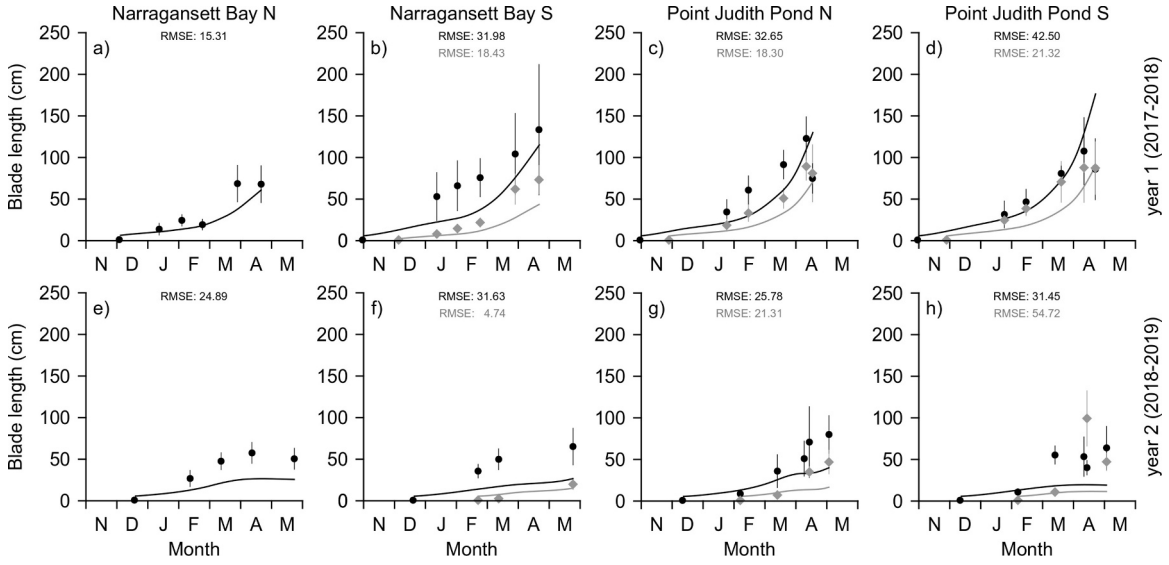

Fig. 7. *Saccharina latissima* blade length (cm) during year 1 (top row) and year 2 (bottom row). Dots and diamonds with error bars depict the mean observed length from the field data and their standard deviation, respectively. Lines are the predicted length from the *S. latissima* DEB model. Lines and dots in black are the first *S. latissima* line planted at a site, and lines and diamonds in grey depict the second *S. latissima* line planted later in the year.

Table 4
Length of *S. latissima* blades in cm (± SD) at the end of the growing season in each site.

Site	Year 1	Year 2
Narragansett Bay North	67.9 (± 22.6)	50.5 (± 13.0)
Narragansett Bay South, Line 1	133.4 (± 78.8)	65.3 (± 22.5)
Narragansett Bay South, Line 2	73.2 (± 17.6)	20.0 (± 6.8)
Pt. Judith Pond North, Line 1	74.8 (± 18.3)	80.1 (± 23.1)
Pt. Judith Pond North, Line 2	81.0 (± 34.8)	46.9 (± 14.7)
Pt. Judith Pond South, Line 1	85.9 (± 37.1)	63.8 (± 26.3)
Pt. Judith Pond South, Line 2	87.3 (± 32.0)	47.1 (± 10.9)

to the field length data ranged widely from 4.74 to 53.72 cm (Fig. 7). Examining the reject fluxes from the growth SU indicate that the C reserve (carbohydrates) limited model growth after planting for greatly variable time spans across the sites, seasons, and lines (Fig. 8). A growth limitation by C reserve may result from low C assimilation due to a low specific relaxation rate. Temperature seemed to be the main factor controlling C assimilation, as indicated by the greater similarity of the shape of the temperature correction to that of C assimilation than the shape of the seasonal trend of irradiance (Fig. 9). N limitation seemed to have a strong role in controlling modeled *S. latissima* growth dynamics overall due to the proportion of time C was rejected from the growth SU.

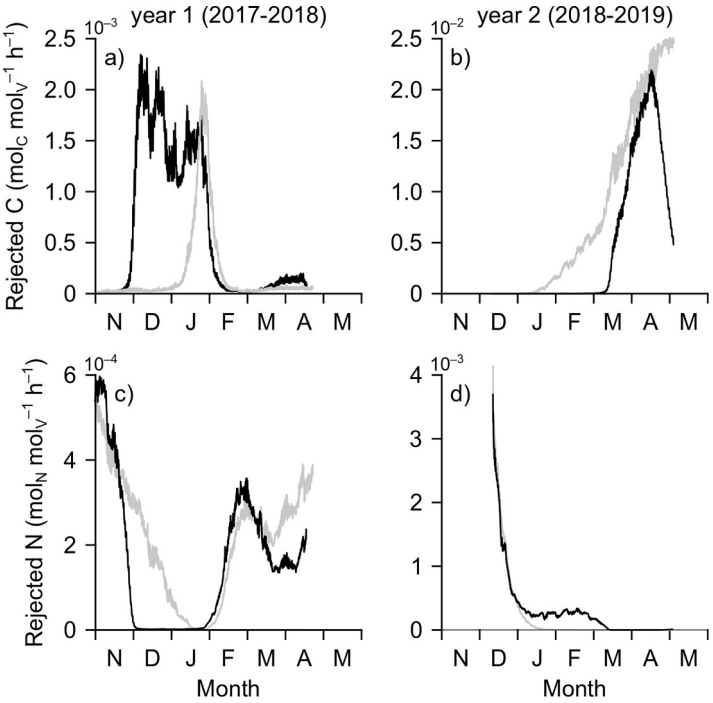

Fig. 8. Rejected fluxes of C (a,b) and N (c,d) from the growth SU back to reserves at Pt. Judith Pond in year 1 (left panels) and year 2 (right panels). Black is for the North *S. latissima* line 1 and the grey is for the South line 1 on all plots.

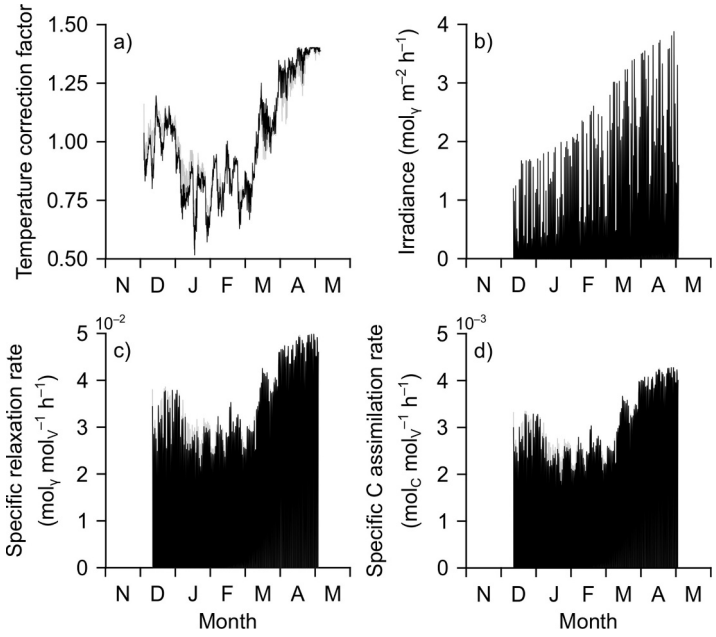

Fig. 9. Temperature correction factor (a), irradiance (b), specific relaxation rate from photosynthetic SU2 (c) and carbon assimilation rate resulting from photosynthetic SU3 (d) at Pt. Judith Pond during year 2. Black is for the North *S. latissima* line and the grey is for the South line.

3.4. Sensitivity analysis

The parameters with the largest effects (>9000 L1 summary value of sensitivity functions) on the state variables were T_0, T_A, T_H, T_L, T_{AH}, T_{AL}, y_{E_CV}, κ_{E_i}, y_{IC}, y_{CO_2C}, and α_I (Fig. 10). The parameters J_{E_CAm}, ρ_{PSU} and $\dot{b}_I$ had a moderate effect with L1 values ranging between 3000-7000. Finally, some parameters showed small but non-zero effects on the state variables, including: y_{E_NV}, $\dot{k}_{EC}$, k_{EN}, j_{CO_2m}, and $\dot{k}_I$ (Fig. 10).

4. Discussion

Aquaculture development represents a key role in expanding U.S. sustainable food production and macroalgae can provide high returns

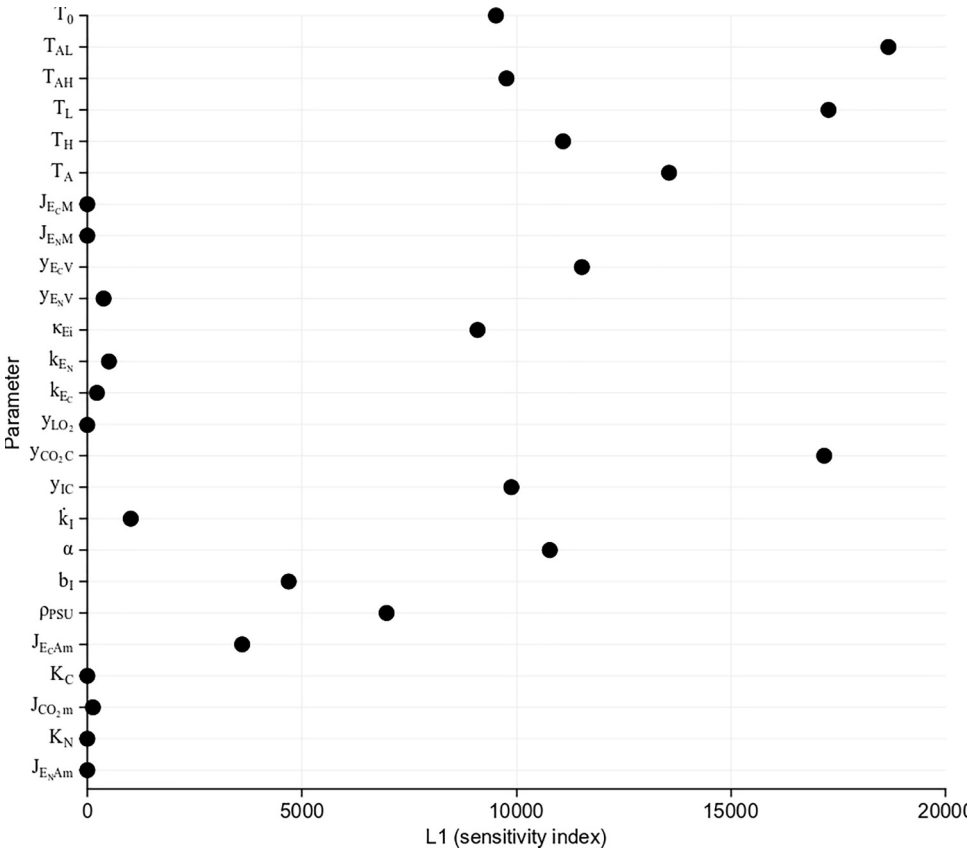

Fig. 10. Results of the sensitivity analysis of the state variables $\boldsymbol{m_{E_C}}$, $\boldsymbol{m_{E_N}}$, and $\boldsymbol{M_V}$ to model parameters as measured by the L1 sensitivity function.

when the proper growth conditions exist. Understanding and predicting the growth dynamics of *S. latissima* can provide the aquaculture industry with a powerful predictive tool for estimating production potential. This model is the first attempt to apply Dynamic Energy Budget (DEB) theory to a macroalga of the order Laminariales. The process-based model presented in this study allowed us to better understand growth limitations as they relate to the behavior of the model.

4.1. Growth limitation

In several model simulations, predictions of early *S. latissima* growth seemed to indicate a limitation in carbon (C) assimilation due to a low modeled specific relaxation rate, $\dot{j}_I$, by photosynthetic SU2 processing the light-dependent reactions of photosynthesis. There is some evidence that a lack of C reserve occurs in the field during winter due to lower irradiance; *S. latissima* individuals older than a year were shown to have a decrease in blade C content mid-winter suggesting consumption of stored carbohydrates (Sjøtun, 1993). New sporophytes would not have this carbohydrate pool to draw upon and would exclusively depend on photosynthesis to acquire C. The decrease in C content observed by Sjøtun (1993) suggests that C dynamics may be limiting *S. latissima* growth, but substrate limitation was not directly examined by this author. In simulations where irradiance was the initial limiting factor for growth, the early season model underestimation of field growth may reflect an outsized impact of the temperature correction of $\dot{k}_I$ on the specific relaxation rate, $\dot{j}_I$, in comparison to irradiance. As with many DEB parameters, $\dot{k}_I$ is difficult to estimate directly based on empirical data and our assumption of dependence on temperature as in other algae (Kooijman, 2010; Lavaud et al., 2020) may not be as relevant to *S. latissima*. As ocean temperature seasonal trends trail behind irradiance changes (Brady-Campbell et al., 1984), *S. latissima*'s early season growth could be driven by this early season increase in irradiance rather than water temperature change. More data are necessary to confirm why the *S. latissima* DEB model underestimates winter growth.

Other than an increase in irradiance, day length could also impact seasonal growth patterns. Broch and Slagstad's (2012) *S. latissima* model used the rate of change of day length in a photoperiodic effect function to mimic growth seasonality. These authors relied on the hypothesis that *S. latissima* is a "seasonal anticipator" with endogenous circadian rhythms (Kain, 1989). Seasonal anticipators are posited to grow strategically in response to a trigger. Other kelps such as *Laminaria hyperborea* and *Laminaria digitata* have been shown to have free-running seasonal growth patterns, which suggests control by endogenous circadian rhythms (Schaffelke and Lüning, 1994). Species-specific evidence for this circadian hypothesis is lacking including the mechanism for what would trigger *S. latissima*'s photoperiodic response. If this is the case, substrate uptake or reserve mobilization parameters may be adjusted in the model in response to a trigger to temporarily favor early winter growth.

Another possible reason for underestimation of early season C dynamics may be a lack of energy gain at night. *S. latissima*'s carbon dioxide exchange rate is not closely correlated with irradiance because carbon dioxide uptake by the alga continues into the dark (Mortensen, 2017). On average, 11% of *S. latissima*'s carbon fixation happens in the dark (Kremer and Markham, 1979). The linkage between the light-dependent and light-independent reactions is modeled in our study as an immediate transference. In other words, when there is no irradiance input, the assimilation of carbohydrates to the C reserve is zero. However, adding this layer of physiological accuracy could reduce model efficiency without increasing predictive capacity.

In some instances, N was the limiting factor to growth, as shown by more rejected C by the growth SU, for example, in Pt. Judith Pond sites in Dec and Jan of year 1, resulting in lower predicted length as compared to field observations. The low resolution of N forcing could limit our interpretation of the results, but our N data show general agreement with long-term monitoring at the University of Rhode Island Graduate School of Oceanography (Reed and Oviatt, 2020). The seasonal dynamics of N in Narragansett Bay matches that of many sites around New England with higher concentrations of N in the October-March and reduced summer N concentrations (Townsend, 1991, Reed and Oviatt, 2020). Nitrogen has been well-documented as a major force limiting primary production across the ocean (Duce et al., 2008). N limitation of *S. latissima* growth may be a reasonable expectation later in the year as inorganic N availability is thought to facilitate late winter and early spring *S. latissima* growth (Ahn et al., 1998).

To increase the ability to accurately understand growth limitation with this DEB model, localized N uptake data in response to changing N concentrations would be useful. Ecotypic differences in N nutrition have been observed both in Nova Scotia (Canada, Espinoza and Chapman, 1983) and when comparing Long Island Sound (New York) kelps with kelps from Maine (Gerard, 1997). In this study, Espinoza and Chapman's (1983) N uptake data from St. Margaret's Bay was chosen for calibration over their Bay of Fundy data because the April-November seasonal depletion of nitrate was more similar to Narragansett Bay conditions than the year-round nitrate replete conditions of the Bay of Fundy. Kelp individuals from St. Margaret's Bay also had greater nitrate accumulation ability (Espinoza and Chapman, 1983). The seasonal dissolved inorganic nitrogen patterns were comparable for the Long Island Sound and Maine kelps that Gerard (1997) analyzed, but the Long Island Sound plants (geographically closer to our kelp from Narragansett Bay) accumulated larger N reserves, which allowed for a ramping up of photosynthetic component production. Such ability to store nitrogen over winter months has been documented (Nielsen et al., 2014) and may explain the observed pattern of C reserve limitation in our model. Year-long simulations would most likely provide different conclusions when N availability in the environment decreases (Reed and Oviatt, 2020).

The chemical composition of available N for assimilation may have an effect on N limitation. Nitrate was the primary N source used in this model primarily due to lack of complete ammonium data to include in the forcing. Including ammonium, however, may allow for more accurate predictions of growth dynamics as ammonium has been hypothesized to be a more efficient N source for macroalgae especially in low light conditions because it may be assimilated passively through diffusion (Harrison and Hurd, 2001). One argument for leaving out ammonium is to simplify dynamics, as a different substrate composition would require another reserve pool, although pools of different N forms may be combined and uptake rates for different N sources averaged. Another reason is that *S. latissima* has been shown to have a higher maximum uptake of nitrate compared to ammonium: ammonium saturation was observed at concentrations of 10 μM whereas nitrate saturation was not observed until 30 μM (Ahn et al., 1998). The greater variation in nitrate uptake could cause nitrate to have a more important role in shaping *S. latissima* growth dynamics. The caveat to using these rates to understand dynamics broadly is that kelp individuals used in this study came from ammonium rich and nitrate poor habitat (Ahn et al., 1998), which may have some effect on the reported uptake rates.

4.2. Sensitivity analysis

The high sensitivity of the state variables to the temperature related parameters is a logical outcome of the central role of temperature in DEB theory. Since the temperature correction is applied to such a large number of rates in the organism, the high sensitivity to these values is reasonable. It is also an argument for caution in regional calibration of the Arrhenius relationship. The sensitivity of the *S. latissima* model to the fraction of rejection flux incorporated back in i-reserve (κ_{Ei}) contrasts with the lack of sensitivity of Lorena et al. (2010)'s microalgae model to the same parameter. Different metabolic pathways, storage capacities, and efficiencies might be responsible for these differences between a phytoplankton species and a macroalgae. More experimental

work focusing on the dynamics of internal and external N concentration in controlled settings should help confirm the calibration of this parameter. The sensitivity of the model to the yield factor of C reserve on photons and on CO_2 (y_{IC} and y_{CO_2C} respectively), reflects the generality of photosynthesis reactions; a change in these parameters would involve important modifications of the physiological processes involved in photosynthesis. Since these processes are well known and established, it reinforces our confidence in the model. The high sensitivity of the model to the yield factor of C reserve to structure (y_{E_CV}) in comparison to the small but nonzero impact of the yield factor of N reserve to structure (y_{E_NV}) might be reflective of the greater amount of C reserve required by the chemical composition of the structure. This greater proportion of C may also be the reason the majority of the impactful parameters are related to C dynamics. The state variables had a small sensitivity to reserve turnover parameters, which calibration may be challenging due to the difficulty to relate these abstract parameters to observed data. It is, therefore, encouraging that the sensitivity to these values was low. This analysis should increase our overall confidence in the values of the calibrated parameters and the reliability of the model as the most sensitive parameters are those in which we can have highest assurance.

4.3. Model application

Limitations to broader geographic use of this parameter set center around the plasticity of *S. latissima* and the existence of ecotypes in this species. The differentiation of ecotypes occurs when individuals have an acclimation range related to their habitat of origin (Gerard, 1988). For instance, *S. latissima* individuals from New York have been shown to have a different physiological response to temperature in a lab setting than individuals from Maine (Gerard, 1988). In the context of this study, Narragansett Bay (RI, U.S.A.) is located towards the southern boundary of *S. latissima* distribution range (Taylor, 1972); kelps from this location likely have different physiological rates than in northern neighboring states. The existence of multiple ecotypes of this species suggests that some parameters, such as the temperature parameters or maximum assimilation rates of substrates, require regional adjustment, particularly in the Arctic. Additionally, the model assumption regarding the proportionality of surface area to volume impedes prediction of blade shape plasticity, which is a characteristic of *S. latissima* related to drag (Buck and Buchholz, 2005). Since the blade thickness and amount of blade ruffling could impact the relationship between surface area and volume, some adjustments to the model may be warranted in regions where blade plasticity results in thicker thalli as the surface area to volume relationship would be impacted. Determining a mechanism for how blade type changes in response to hydrodynamic conditions would provide a clearer picture of overall growth dynamics.

Further research on the mechanisms for frond loss, blade plasticity, and regional parameter information have the potential to improve this DEB model. A better understanding of the physiological cause for apical frond loss would allow this process to be included in mechanistic models in a more meaningful way than modeling erosion as a response to one correlated variable such as length or age. Aging mechanisms within DEB theory (Kooijman, 2010), based on the production of harmful compounds may also be of interest to model frond loss. Finally, underwater carbon dioxide uptake data and more regionally appropriate oxygen production data in response to variable irradiance would be useful to better calibrate parameters linked to *S. latissima* photosynthesis.

Our model establishes a baseline for *S. latissima* DEB parameters and further testing of the model equations from Lavaud et al. (2020). This tool facilitates analyzing local growth limitations as they relate to modeled responses to changing environmental conditions. Our *S. latissima* DEB model is a first step towards estimating kelp aquaculture production in the U.S.A. In future work, this *S. latissima* DEB model could be coupled with a DEB model for *C. virginica* (Lavaud et al., 2017) and the Regional Ocean Modeling System (ROMS) with a Carbon Silicate Nitrogen Ecosystem (CoSiNE) model (Chai et al, 2009) to predict growth potential at sites in the Northeastern U.S.A. Supporting macroalgae aquaculture is an important avenue to work towards the vital goals of feeding a growing human population and while combatting climate change.

Author statement

Celeste T. Venolia: Conceptualization, Methodology, Formal analysis, Validation, Visualization, Data curation, Writing – Original Draft, Writing – Review & Editing

Romain Lavaud: Conceptualization, Software, Methodology, Visualization, Writing – Original Draft, Writing – Review & Editing

Lindsay A. Green-Gavrielidis: Funding acquisition, Supervision, Investigation, Conceptualization, Data curation, Writing – Original Draft, Writing – Review & Editing

Carol Thornber: Funding acquisition, Supervision, Resources, Writing – Original Draft, Writing – Review & Editing

Austin T. Humphries: Funding acquisition, Supervision, Resources, Project administration, Conceptualization, Methodology, Writing – Original Draft, Writing – Review & Editing

Funding

This work is supported by a National Oceanic and Atmospheric Administration Saltonstall-Kennedygrant [17GAR008], NSERC grant [497065-2016], the National Science Foundation under EPSCoR Cooperative Agreement #OIA-165522 and the U.S. Department of Agriculture's National Institute of Food and Agriculture, Hatch Formula project 1011478.

Declaration of competing interest

The authors declare that they have no known competing financial interests or personal relationships that could have appeared to influence the work reported in this paper.

Acknowledgements

This study would not have been possible without the valuable contributions of the aquaculture farmers working with us to grow kelp for two years: Cindy and John West of Moonstone Oysters, Russ and Thomas Blank of Rome Point Oyster Farm, Trip Whilden of Wickford Oyster Co, and Perry Russo of Matunuck Oyster Farm. Dave Ullman and Chris Kincaid provided assistance in the initial project development. Thomas Guyondet facilitated collaborations around this project. Dawn Outram at the Marine Science Research Facility at URI's Narragansett Bay Campus and Kelly Addy conducted water analyses. Candace Oviatt and Laura Reed shared their nitrogen data, which is funded by EPA, NOAA-CHRP and RI DEM. T. Ben-Horin provided assistance collecting reproductive kelp. J. Barnes, A. Barry, R. Derouin, E. Ferrante, I. Gray, K. Hannibal, C. Jenkins, A. Mauk, L. Sebesta, and A. Wetzel provided lab and field assistance. S. McWilliams, D. Ullman, M. Gomez-Chiarri, L. Josephs, and K. Gorospe provided feedback on previous versions of the manuscript.

References

Ahn, O., Petrell, R.J., Harrison, P.J., 1998. Ammonium and nitrate uptake by *Laminaria saccharina* and *Nereocystis luetkeana* originating from a salmon sea cage farm. J. Appl. Phycol. 10 (4), 333–340.

Alleway, H.K., Gillies, C.L., Bishop, M.J., Gentry, R.R., Theuerkauf, S.J., Jones, R., 2019. The ecosystem services of marine aquaculture: valuing benefits to people and nature. Bio. Sci. 69 (1), 59–68.

Axelsson, L., Mercado, J., Figueroa, F., 2000. Utilization of HCO_3^- at high pH by the brown macroalga *Laminaria saccharina*. Eur. J. Phycol. 35 (1), 53–59.

Boden, G.T., 1979. The effect of depth on summer growth of *Laminaria saccharina* (Phaeophyta, Laminariales). Phycologia 18 (4), 405–408.
Bolton, J.J., Lüning, K., 1982. Optimal growth and maximal survival temperatures of Atlantic *Laminaria* species (Phaeophyta) in culture. Mar. Biol. 66 (1), 89–94.
Brady-Campbell, M.M., Campbell, D.B., Harlin, M.M., 1984. Productivity of kelp (*Laminaria* spp.) near the southern limit in the northwestern Atlantic Ocean. Mar. Ecol. Prog. Ser. 18 (1), 79–88.
Broch, O.J., Slagstad, D., 2012. Modelling seasonal growth and composition of the kelp *Saccharina latissima*. J. Appl. Phycol. 24 (4), 759–776.
Brown, M.T., Nyman, M.A., Keogh, J.A., Chin, N.K.M., 1997. Seasonal growth of the giant kelp *Macrocystis pyrifera* in New Zealand. Marine Biology 129 (3), 417–424.
Buchholz, C., Lüning, K., 1999. Isolated, distal blade discs of the brown alga *Laminaria digitata* form sorus, but not discs, near to the meristematic transition zone. J. Appl. Phycol. 11 (6), 579.
Buck, B.H., Buchholz, C.M., 2005. Response of offshore cultivated *Laminaria saccharina* to hydrodynamic forcing in the North Sea. Aquaculture 250 (3-4), 674–691.
Chai, F., Liu, G., Xue, H., Shi, L., Chao, Y., Tseng, C.-M., Chou, W.-C., Liu, K.-K., 2009. Seasonal and interannual variability of carbon cycle in South China Sea: a three-dimensional physical-biogeochemical modeling study. J. Oceanogr. 65, 703–720.
Cho, C.Y., Bureau, D.P., 1998. Development of bioenergetic models and the Fish-PrFEQ software to estimate production, feeding ration and waste output in aquaculture. Aquat. Living Resour. 11 (4), 199–210.
Dame, R.F., 1972. The ecological energies of growth, respiration and assimilation in the intertidal American oyster *Crassostrea virginica*. Mar. biol. 17 (3), 243–250.
Davison, I.R., 1987. Adaptation of photosynthesis in *Laminaria saccharina* (Phaeophyta) to changes in growth temperature. J. Phycol. 23, 273–283.
Davison, I.R., Davison, J.O., 1987. The effect of growth temperature on enzyme activities in the brown alga *Laminaria saccharina*. Br. Phycol. J. 22 (1), 77–87.
Denny, M., Helmuth, B., 2009. Confronting the physiological bottleneck: a challenge from ecomechanics. Integr. Comp. Biol. 49 (3), 197–201.
Duarte, C.M., Wu, J., Xiao, X., Bruhn, A., Krause-Jensen, D., 2017. Can seaweed farming play a role in climate change mitigation and adaptation. Front. Mar. Sci. 4, 100.
Duce, R.A., LaRoche, J., Altieri, K., Arrigo, K.R., Baker, A.R., Capone, D.G., ..., Geider, R.J., 2008. Impacts of atmospheric anthropogenic nitrogen on the open ocean. Science 320 (5878), 893–897.
Eaton, A.D., Clesceri, L.S., Greenberg, A.E., Franson, M.H., 1998. Standard Methods For The Examination Of Water And Wastewater. APHA, AWWA, and WEF, Washington, DC.
Espinoza, J., Chapman, A.R.O., 1983. Ecotypic differentiation of *Laminaria longicruris* in relation to seawater nitrate concentration. Mar. Biol. 74 (2), 213–218.
FAO, 2018. The State of World Fisheries and Aquaculture 2018 - Meeting The Sustainable Development Goals. Licence: CC BY-NC-SA 3.0 IGO, Rome.
Filgueira, R., Guyondet, T., Comeau, L.A., Grant, J., 2014. A fully-spatial ecosystem-DEB model of oyster (*Crassostrea virginica*) carrying capacity in the Richibucto Estuary, Eastern Canada. J. Mar. Syst. 136, 42–54.
Forbord, S., Skjermo, J., Arff, J., Handå, A., Reitan, K.I., Bjerregaard, R., Lüning, K., 2012. Development of *Saccharina latissima* (Phaeophyceae) kelp hatcheries with year-round production of zoospores and juvenile sporophytes on culture ropes for kelp aquaculture. J. Appl. Phycol. 24 (3), 393–399.
Fortes, M.D., Lüning, K., 1980. Growth rates of North Sea macroalgae in relation to temperature, irradiance and photoperiod. Helgoländer Meeresuntersuchungen 34 (1), 15.
Froehlich, H.E., Afflerbach, J.C., Frazier, M., Halpern, B.S., 2019. Blue growth potential to mitigate climate change through seaweed offsetting. Curr. Biol. 29, 1–7.
Gagné, J.A., Mann, K.H., Chapman, A.R.O., 1982. Seasonal patterns of growth and storage in *Laminaria longicruris* in relation to differing patterns of availability of nitrogen in the water. Mar. Biol. 69 (1), 91–101.
Gevaert, F., Davoult, D., Creach, A., Kling, R., Janquin, M.A., Seuront, L., Lemoine, Y., 2001. Carbon and nitrogen content of *Laminaria saccharina* in the eastern English channel: biometrics and seasonal variations. J. Mar. Biol. Assoc. United Kingdom 81 (5), 727–734.
Gerard, V.A., 1988. Ecotypic differentiation in light-related traits of the kelp *Laminaria saccharina*. Mar. Biol. 97 (1), 25–36.
Gerard, V.A., 1997. The role of nitrogen nutrition in high-temperature tolerance of the kelp, *Laminaria saccharina* (Chromophyta). J. Phycol. 33 (5), 800–810.
Grant, J., Curran, K.J., Guyondet, T.L., Tita, G., Bacher, C., Koutitonsky, V., Dowd, M., 2007. A box model of carrying capacity for suspended mussel aquaculture in Lagune de la Grande-Entrée, Iles-de-la-Madeleine, Québec. Ecol. model. 200 (1-2), 193–206.
Handå, A., Forbord, S., Wang, X., Broch, O.J., Dahle, S.W., Størseth, T.R., ..., Skjermo, J., 2013. Seasonal-and depth-dependent growth of cultivated kelp (*Saccharina latissima*) in close proximity to salmon (*Salmo salar*) aquaculture in Norway. Aquaculture 414, 191–201.
Harrison, P.J., Hurd, C.L., 2001. Nutrient physiology of seaweeds: application of concepts to aquaculture. Cahiers De Biol. Mar. 42 (1-2), 71–82.
Heinrich, S., Valentin, K., Frickenhaus, S., John, U., Wiencke, C., 2012. Transcriptomic analysis of acclimation to temperature and light stress in *Saccharina latissima* (Phaeophyceae). PLoS One 7 (8), e44342.
Herbeck, L.S., Unger, D., Wu, Y., Jennerjahn, T.C., 2013. Effluent, nutrient and organic matter export from shrimp and fish ponds causing eutrophication in coastal and back-reef waters of NE Hainan, tropical China. Cont. Shelf Res. 57, 92–104.
Johansson, G., Snoeijs, P., 2002. Macroalgal photosynthetic responses to light in relation to thallus morphology and depth zonation. Mar. Ecol. Prog. Ser. 244, 63–72.
Kain, J.M., 1989. The seasons in the subtidal. Br. Phycol. J. 24 (3), 203–215.
Kooijman, S.A.L.M., 2010. Dynamic Energy Budget Theory For Metabolic Organisation. Cambridge university press.
Kremer, B.P., Markham, J.W., 1979. Carbon assimilation by different developmental stages of *Laminaria saccharina*. Planta 144 (5), 497–501.
Krumhansl, K.A., Lauzon-Guay, J.S., Scheibling, R.E., 2014. Modeling effects of climate change and phase shifts on detrital production of a kelp bed. Ecology 95 (3), 763–774.
LACHAT, 2008. QuikChem Method 31-107-04-1-A. LACHAT INSTRUMENTS, Loveland, CO.
Lavaud, R., La Peyre, M.K., Casas, S.M., Bacher, C., La Peyre, J.F., 2017. Integrating the effects of salinity on the physiology of the eastern oyster, *Crassostrea virginica*, in the northern Gulf of Mexico through a dynamic energy budget model. Ecol. Model. 363, 221–233.
Lavaud, R., Filgueira, R., Nadeau, A., Steeves, L., Guyondet, T., 2020. A dynamic energy budget model for the macroalga *Ulva lactuca*. Ecol. model. 418, 108922.
Livanou, E., Lagaria, A., Psarra, S., Lika, K., 2019. A DEB-based approach of modeling dissolved organic matter release by phytoplankton. J. Sea Res. 143, 140–151.
Lorena, A., Marques, G.M., Kooijman, S.A.L.M., Sousa, T., 2010. Stylized facts in microalgal growth: interpretation in a dynamic energy budget context. Philos. Trans. R. Soc. B: Biol. Sci. 365 (1557), 3509–3521.
Lüning, K., Wagner, A., Buchholz, C., 2000. Evidence for inhibitors of sporangium formation in *Laminaria digitata* (Phaeophyceae) during the season of rapid growth. J. Phycol. 36 (6), 1129–1134.
Mesinger, F., DiMego, G., Kalnay, E., Mitchell, K., Coauthors, 2006. North American regional reanalysis. Bull. Am. Meteorol. Soc. 87, 343–360.
Mortensen, L.M., 2017. Diurnal carbon dioxide exchange rates of *Saccharina latissima* and *Laminaria digitata* as affected by salinity levels in Norwegian fjords. J. Appl. Phycol. 29 (6), 3067–3075.
Mõttus, Matti, Sulev, Madis, Frederic, Baret, Lopez-Lozano, R, Reinart, Anu, 2011. Photosynthetically active radiation: measurement and modeling. In: Meyers, R. (Ed.), Encyclopedia of Sustainability Science and Technology. Springer, New York, NY, pp. 7970–8000.
Muller, E.B., Nisbet, R.M., 2014. Dynamic energy budget modeling reveals the potential of future growth and calcification for the coccolithophore *E miliania huxleyi* in an acidified ocean. Glob. Change Biol. 20 (6), 2031–2038.
National Marine Fisheries Service (2018) Fisheries of the United States, 2017. U.S. department of commerce, NOAA current fishery statistics No. 2017 available at:https://www.fisheries.noaa.gov/feature-story/fisheries-united-states-2017.
Ní Longphuirt, S., Eschmann, C., Russell, C., Stengel, D.B., 2013. Seasonal and species-specific response of five brown macroalgae to high atmospheric CO2. Mar. Ecol. Prog. Ser. 493, 91–102.
Nielsen, M.M., Krause-Jensen, D., Olesen, B., Thinggaard, R., Christensen, P.B., Bruhn, A., 2014. Growth dynamics of *Saccharina latissima* (Laminariales, Phaeophyceae) in Aarhus Bay, Denmark, and along the species' distribution range. Mar. Biol. 161 (9), 2011–2022.
Petrell, R.J., Tabrizi, K.M., Harrison, P.J., Druehl, L.D., 1993. Mathematical model of *Laminaria* production near a British Columbian salmon sea cage farm. J. Appl. Phycol. 5 (1), 1–14.
Poggiale, J.C., Baklouti, M., Queguiner, B., Kooijman, S.A.L.M., 2010. How far details are important in ecosystem modelling: the case of multi-limiting nutrients in phytoplankton–zooplankton interactions. Philos. Trans. R. Soc. Lond. B: Biol. Sci. 365 (1557), 3495–3507.
R Core Team, 2019. R: A Language And Environment For Statistical Computing. R Foundation for Statistical Computing, Vienna, Austria URL. https://www.R-project.org/.
Redmond, S., Green, L.A., Yarish, C., Kim, J., Neefus, C.D., 2014. New England seaweed culture handbook: nursery systems. Conn. Sea Grant Coll. Progr. 92. CTSG-14-01Available at: https://seagrant.uconn.edu/2014/01/01/new-england-seaweed-culture-handbook-nursery-systems/.
Reed, Laura and Candace Oviatt. 2020. Graduate school of oceanography dock data, 1977 to present. [dataset].
Ren, J.S., Stenton-Dozey, J., Plew, D.R., Fang, J., Gall, M., 2012. An ecosystem model for optimising production in integrated multitrophic aquaculture systems. Ecol. Model. 246, 34–46.
Schaffelke, B., Lüning, K., 1994. A circannual rhythm controls seasonal growth in the kelps *Laminaria hyperborea* and *L. digitata* from Helgoland (North Sea). Eur. J. Phycol. 29 (1), 49–56.
Segarra, K.E.A., 2002. Source Or Sink? Analysis of Narragansett Bay's carbon cycle. Brown University. Center for Environmental Studies.
Sjøtun, K., 1993. Seasonal lamina growth in two age groups of *Laminaria saccharina* (L.) Lamour. in western Norway. Bot. Mar. 36 (5), 433–442.
Soetaert, K., Petzoldt, T., 2010. Inverse modelling, sensitivity and Monte Carlo analysis in R using package FME. J. Stat. Softw. 33 (3), 1–28.
Soetaert, K., Petzoldt, T.R., Setzer, W., 2010. Solving differential equations in R: package deSolve. J. Stat. Softw. 33 (9), 1–25. https://doi.org/10.18637/jss.v033.i09. URL. http://www.jstatsoft.org/v33/i09/.
Taylor, W.R., 1972. Marine Algae Of The Eastern Tropical And Subtropical Coasts Of The Americas. University of Michigan.
Townsend, D.W., 1991. Influences of oceanographic processes on the biological

productivity of the Gulf of Maine. Rev. Aquat. Sci. 5 (3), 211–230.
Ullman, D. S. & Codiga, D. L. (2010) *Characterizing the physical oceanography of coastal waters off Rhode Island, Part 2: new observations of water properties, currents, and waves*. Retrieved fromhttps://www.seagrant.gso.uri.edu/oceansamp/pdf/appendix/03-PhysOcPart2-OSAMP-UllmanCodiga2010.pdf.
Vettori, D., Nikora, V., 2017. Morphological and mechanical properties of blades of *Saccharina latissima*. Estuar., Coast. Shelf Sci. 196, 1–9.
Wu, R.S.S., 1995. The environmental impact of marine fish culture: towards a sustainable future. Mar. Pollut. Bull. 31 (4-12), 159–166.